1

Climate and Environmental Modelling

THE C-MMACS ENVIRONMENTAL MODELLING PROGRAMME (CEMP)

Capacity to model and forecast environmental processes at user-specified spatio- temporal scales has the potential to revolutionize our approach and ability to address many issues that concern us closely. It was to address these issues in an integrated manner and to generate a capability for multi-scale forecasting that CEMP was initiated.

Over the years, CEMP has slowly grown in its scope and capability. A multi-pronged approach, involving research in process modelling, model evaluation, forecast methodology and alternative modelling has resulted in several milestones in CEMP.

Inside

A Schematic Representation of CEMP

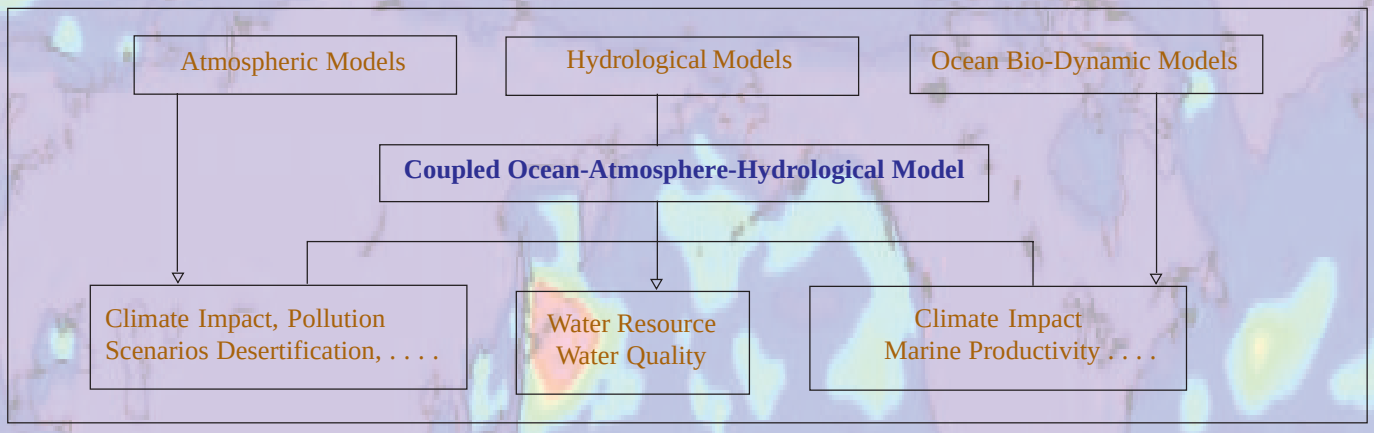

Some Milestones :

The Modular Ocean Model has been installed and evaluated; this paves the way for ocean state forecasting.

A comprehensive dynamical mechanism for the broad spectrum of tropical variabilities has been developed; this has direct implications for model improvement and model evaluation.

A new parameterization of convection in the tropics has been developed using the concept of convective time lag.

A preferred scale for intensification of tropical disturbances has been predicted using numerical experiments; this has direct implications for early identification and early warning of tropical cyclones.

Process models for marine primary productivity have been developed and evaluated. This forms the basis for modelling higher trophic levels.

The Neural Network model developed at C-MMACS for long-range forecasting of monsoon rainfall has been successfully used to generate experimental forecasts for the past seven years.

CEMP : Major National and International Collaborations

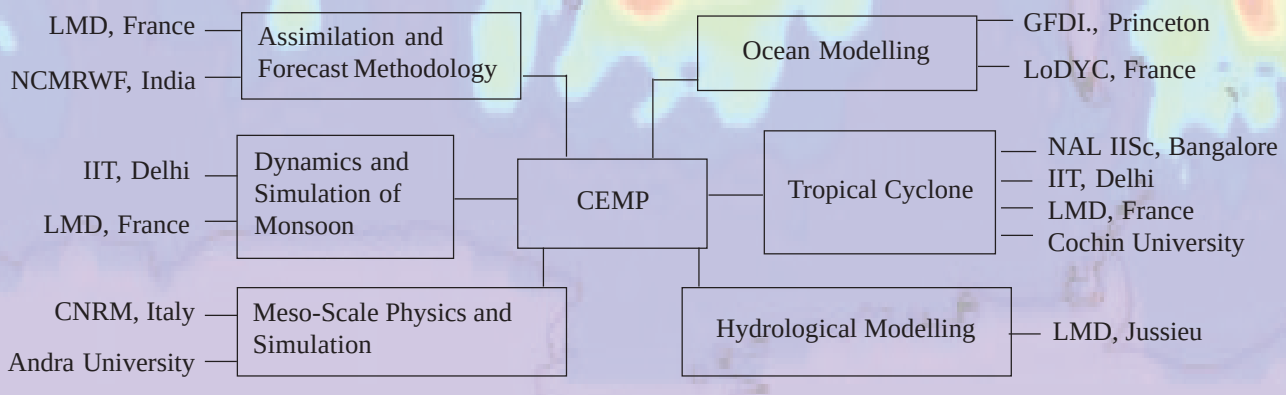

1.1 Variable Resolution GCM Simulation of Tropical Cyclone

Every year, the coastline of India is threatened by the tropical cyclones that develop over the Indian seas. Thanks to a growing population and industrial activity in the coastal areas, each tropical cyclone hitting the coast to-day is a multi-billion rupee threat. Advance and reliable forecasts of these storms therefore can result in much better disaster management, saving life and property. Yet, in spite of a sustained effort by the scientific community the skill of forecast for critical parameters like intensity and track still remain below desired levels.

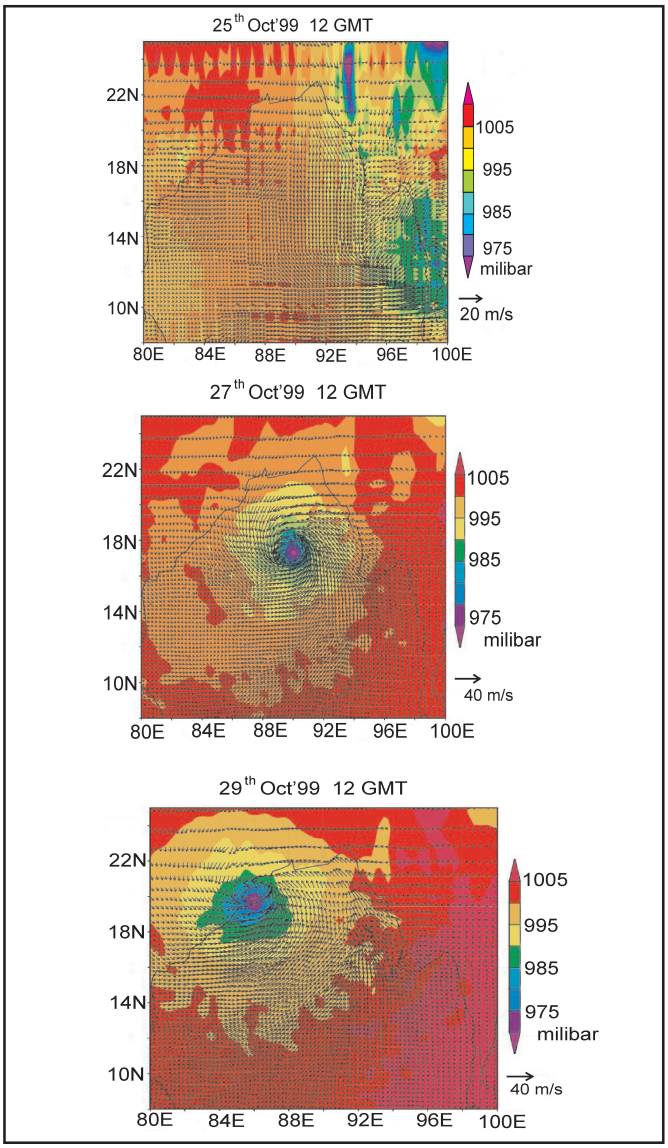

Fig. 1.1 Simulation of october 1999 Orissa super cycone using a variable resolution atmospheric general circulation model. The initial condition, given from ECMWF analysis for october 25, 1999 with no significant cyclone activity over the area. The fields show surface preessure and vector wind.

Traditionally, the modelling tool to simulate and forecast tropical cyclones has been the so called limited area models (LAM) or meso-scale models (MM); three dimensional models of the atmosphere defined over a domain much smaller than the global domain. The advantage of LAM is that it can afford very high resolution over the domain of interest; the disadvantages are that it introduces artificial lateral boundary conditions which have to be supplied externally (as against periodic boundary conditions in a GCM). Besides LAM cannot incorporate the effect of larger (than domain) scale circulations except through the boundary conditions. Yet there is growing evidence that the large scale circulation have considerable effect on the smaller scale circulation.

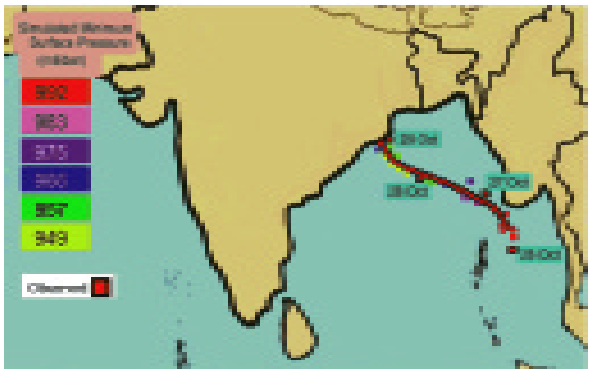

Fig. 1.2 Comparision of the track of the october 1999 Orissa super cyclone from observation (black line) and simulation (colour) using the variable-resolution atmospheric general circulaiton model.

A different strategy has been adopted at C-MMACS, which combines the advantages of a GCM and a LAM to a large extent. This is achieved through adopting a Variable Resolution GCM (VR GCM) which allows a higher resolution (zoom) over a specified domain. The VR GCM adopted by us is the version LMDZ 3.3 developed at the Laboratory for Dynamic Meteorology, Paris. The VR GCM has been successfully applied to simulate monsoon circulation. We have now configured the model to simulate a system with smaller scale viz tropical cyclones.

As a first step towards model evaluation we have applied the VR GCM to simulate the super cyclone that hit the coast of Orissa in October 1999. The initial conditions were adopted from ECMWF Analysis and sea surface temperature was taken from the Atmospheric Model Inter Comparison Project (AMIP) data set, prescribed monthly.

Figure 1.1 shows the model simulations (surface pressure in color and vector wind fields), starting from the initial condition on October 25, 1999 on model grid. The subsequent

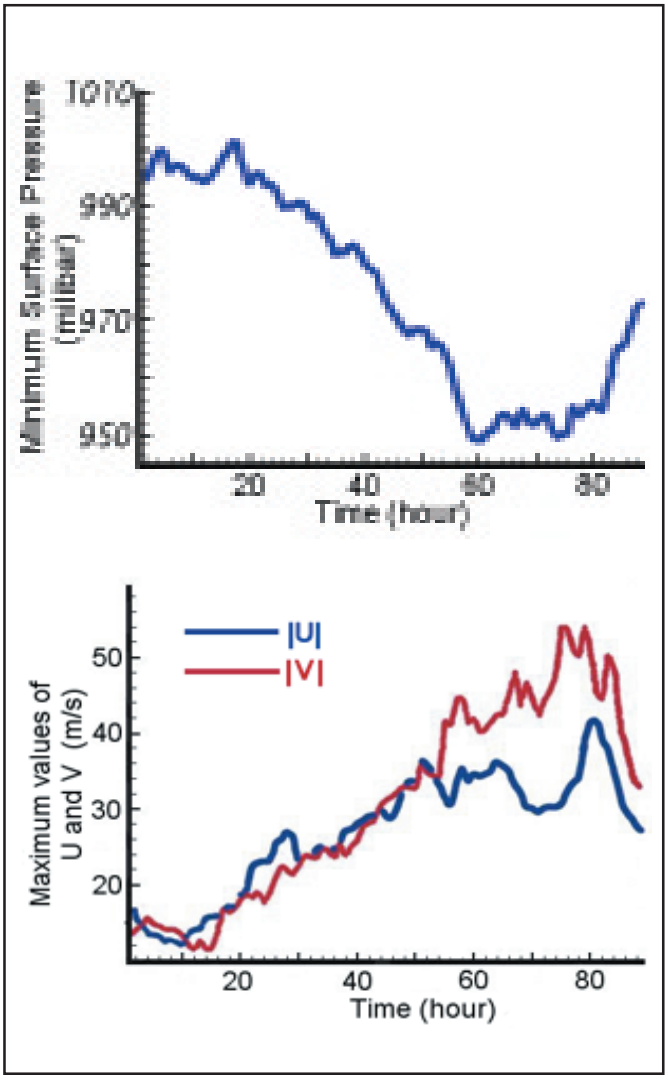

Fig. 1.3 Time evolution of the october 1999 Orissa super cyclone in simulation using a variable-resolution atmospheric general circulation model.

panels in figure 1.1 shows the daily fields from the model simulations for alternate days, until Oct 29, 1999 the day of the landfall for the cyclone. The simulations clearly indicate the west-north-west movement of the cyclone as well as the intensification of the system and subsequent dacay after landfall.

A very important quantity in tropical cyclone forecast is the track of the system. Figure 1.2 compares the simulated track (in colour) with the observed track (black line). Inspite of the very good initial agreement, the simulated location of landfall is somewhat off the observed location. However, the error, about 50 kms, is comparable to the best simulations available from other (LAM and MM) models.

Figure 1.3 shows the growth and decay of the system in terms of minimum surface pressure and maximum wind components attained during the period of simulation. The intensity (minimum surface pressure attained) is somewhat less than the observed value reported.

The C-MMACS effort on tropical cyclone is part of a bigger, ambitious national programme under the New Millenium Indian Technology Leadership Initiative Programme (NMITLI). The studies with VR GCM in general are part of the collaborative programme under Indo-French Centre for Climate and Environment (IFCEC).

(P Goswami, A Mandal)

1.2 Long-Range Forecast of Monsoon Rainfall

The amount and distribution of rainfall is a decisive factor in many aspects like agricultural production and availability of ground water. For several countries including India, and thus for a significant fraction of the world population, this rainfall is primarily determined by the (summer) monsoon, the large-scale precipitation that accompanies the seasonal reversal of the winds. Thus accurate, long-range prediction of rainfall pattern can contribute significantly towards advance and improved planning of agricultural strategy (crop selection, planting schedule, irrigation requirement etc.) and crisis (e.g drought) preparedness. However, in spite of considerable efforts, successful long-range prediction of monsoon rainfall still remains elusive, especially at longer than seasonal scales.

An important and widely used measure of performance of the Indian summer monsoon (June to September) is the all-India mean summer monsoon rainfall (hereafter ISMR). Most of the studies aimed at long-range statistical prediction of ISMR attempt at finding suitable predictor parameters. The resulting forecast equations are generally either regression relations or power regression relations with one or more predictors. However, quite often many of the required predictions are not available well in advance, such as in the case of ISMR. Therefore the use of this method for prediction of ISMR in longer than a season in advance is limited. Besides, the statistical relationships between most of these predictors undergo low frequency changes, which reduce their reliability over long periods of time. This is particularly true for prediction for longer than a season in advance. Although some of the statistical models have shown considerable skill in forecasting Indian summer monsoon rainfall (ISMR),

their range does not exceed a few months. Besides, most of these statistical (regression) models require a number of observed parameters many of which are not available until before onset. This has been one of the major obstacles in attempts to generate very long range (VLR, one year or more) forecasting of monsoonal rainfall.

In recent years, another modelling technique, known as artificial neural networks (NN), has become popular as an alternative tool for modelling and prediction of complex time series in general, and of weather and climate variables in particular.

An attempt at VLR forecast of ISMR was made at C-MMACS using neural networks. While, a large number of experiments revealed conventional NN to have rather poor skill at predicting ISMR by themselves, However, a generalization NN, termed cognitive network, was found to have potential for generating VLR forecast of ISMR with good accuracy.

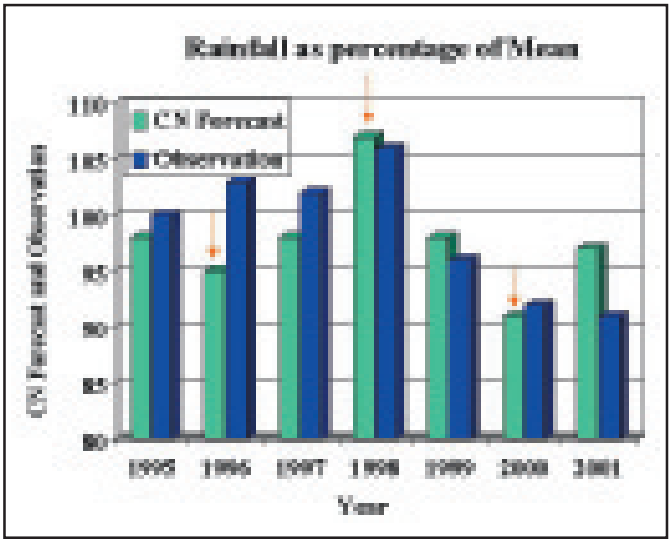

Fig. 1.4 Comparision of experimental forecasts of all-India summer monsoon rainfall using cognitive network with observation. The 2-year forecast represent forecasts two seasons in advance.

Cognitive networks have proved to be successful tool for generating long-range forecasts of ISMR, as shown by a large number of hindcast experiments. Encouraged by these results, C-MMACS has been generating experimental forecasts of ISMR since 1995 well ahead of the season, several times two seasons in advance. Figure 1.4 compares the CN forecasts with actual observation for the past seven years. These experimental forecasts can provide an objective estimate of the skill of the forecasts. It should be emphasized, however, that these forecasts are purely experimental one, to provide an objective evaluation of the forecast skill of our method; they are thus not meant for any operational or commercial use.

With this philosophy we record here our experimental forecasts of ISMR for 2002 and 2003: ISMR in mm, ISMR as % of long period mean.

The continued success of CN forecasts for the last seven years is encouraging; it is a remarkable and significant fact that the CN model uses only past rainfall as its predictor. On the other hand, none of the past six years was a major deviation from normal monsoon, the biggest deviation being in the year 2000 by about 8% (which the CN predicted correctly); thus the skill of CN in forecasting large departures is yet to be tested in the field.

(P Goswami)

1.3 Intraseasonal Variability of Sea Surface Temperature in an OGCM

In addition to a very clear variability at the seasonal timescale, associated with the Indian monsoon, The Indian Ocean also displays variability at intraseasonal and interannual timescales, While there has been a number of works on the interannual variabities, the variabilities at sub-seasonal scales have not received as much attention. In view of paucity of data with adequate spatio-temporal resolution and coverage, simulations from state-of-the-art models provide an excellent alternative. We have used existing model simulations (OPA-Model) to study the Indian Ocean SST variabilities at intra-seasonal scale over the Indian Ocean.

The Ocean General Circulation Model (OGCM) used here is OPA-8; (http://www.lodyc.jussieu.fr/opa/). This model is based on the primitive equations, including currents, potential temperature and salinity. The simulation has used a horizontal grid of resolution 2^o in longitude and latitudinal resolution of 0.5^o at the equator to about 2° at 20^oN. There are 31 vertical levels with the highest resolution (10 m) in the upper 150 m and the time step is 1 hour 36 minutes. The vertical mixing coefficients are computed based on a 1.5 turbulent closure scheme. This scheme permits an explicit formulation of the mixed layers as well as a minimum diffusion in the thermocline. An isopycnal mixing is used on both momentum and active tracers with eddy coefficient of 2000 m^2s^{-1}.

We have used outputs from two different experiments with various forcings for our studies. In experiment-(Expt-1) surface fluxes of momentum, heat and freshwater were

specified. The wind stress was taken from ERS1-2 weekly wind stress. The surface heat and fresh water fluxes have been taken from the daily NCEP reanalysis. The solar and non-solar components of the heat flux were specified separately, in order to allow the heating associated with the penetrative solar flux to be accounted for. The non-solar flux term includes a relaxation to Reynolds and Smith (1994) weekly SST product, with a –40 $Wm^{-2}K^{-1}$ coefficient. This experiment was integrated for the period 1993-1999. In experiment-2, the wind forcing is same as in EXPT-1, but the heat and surface fluxes are computed using bulk formulae on a global grid.

Fig. 1.5 shows the RMS map of high pass filtered model and TMI SST variability. This shows that the model results strongly underestimate the SST variability at intraseasonal timescale in both experiments. This is especially striking in the experiment using the bulk formulas (not shown). In Expt-1, this could be due to the relaxation to Reynolds SST which has a 45 days relaxation timescale for a 40-m thick layer, and that might damp the model SST variability at intraseasonal timescale. In Expt-2, this is probably due to both to the absence of some important components of the forcing (intraseasonal variations of the solar and latent heat flux) and to a strong damping effect linked to the use of climatological values of the air temperature in the Bulk Formula.

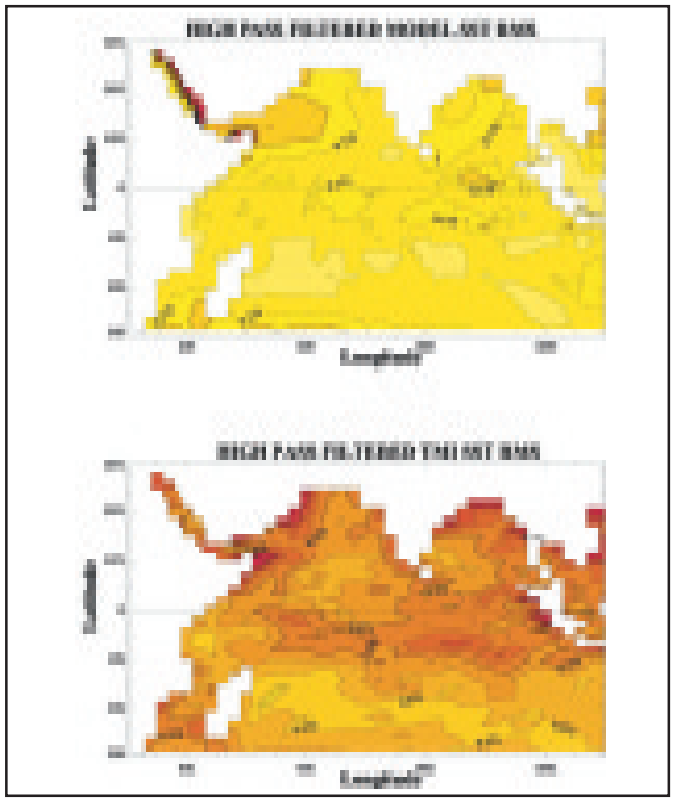

Fig. 1.5 Root mean square of high passed filtered model (Expt-1) and TMI SST.

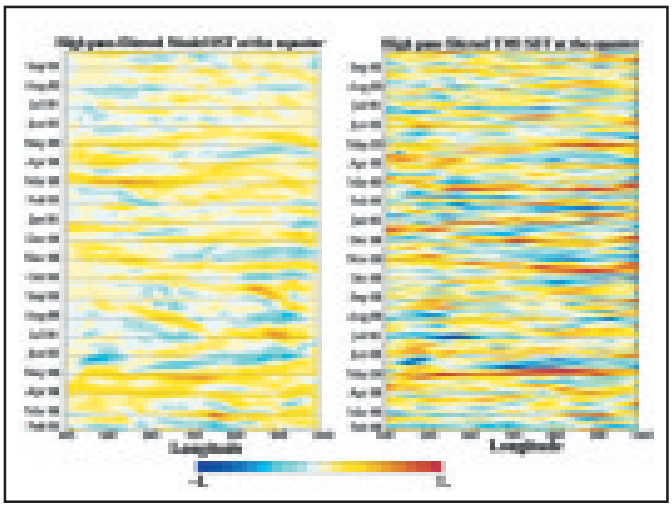

Fig. 1.6 Zonal-time section of model (Expt-1) and TMI high passed filtered SST variability along the equator.

The observations show active zone of SST variability in a region south of the equator in the central and eastern Indian Ocean (65°E-95°E, 10°S-3°, hereafter called SOE) and along the eastern EIO coast and in the northern Bay of Bengal and Arabian Sea regions. The model seems to reproduce an increase of the intraseasonal SST variability in these regions, but with a much smaller amplitude than observed. Fig. 1.6 shows high passed filtered model (Expt-1) and observed (TMI) SST variability for 1998-99. It shows once more that the model underestimates the SST signal. However, there is a good phase agreement between the model and observations (but we should remember here that the model is relaxed to Reynolds SST which retains some of the observed intraseasonal variability).

Fig.1.7 shows the high pass filtered SST, windstress and fluxes over the SOE box for 1998-1999. It is difficult to find any simple relation between the wind, fluxes and SST variability on this plot, which is probably due to the influence of the background seasonal cycle (e.g. an eastward wind anomaly will increase or decrease the fluxes depending on the mean wind direction). However, a few things can be noticed, like the strong coherence of the zonal and meridional variations of the wind stress at intraseasonal timescale in this region (middle pannel). The warming/ cooling observed during the early months 1999 is the biggest in the time series.

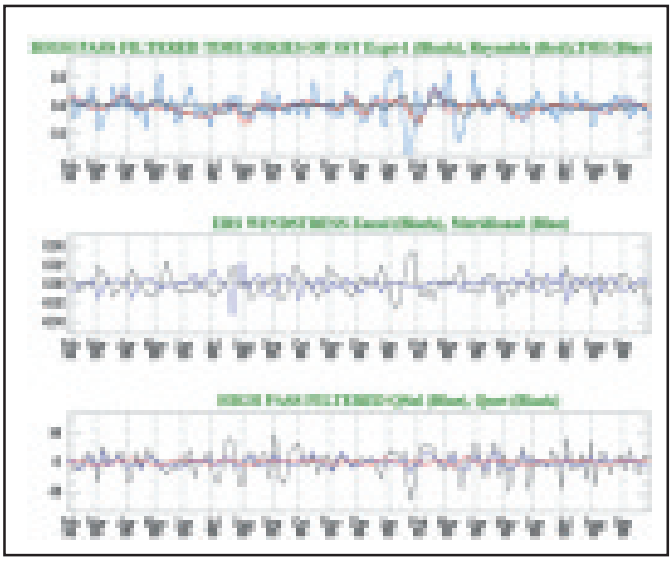

Fig. 1.7 Average high passed filitered time series in the 65^0 –95^0 E and 10^0 S – 3^0 S box (South of the equator) a) Model (Expt-1) and TMI SST, b) ERS windstress and C) Solar and non-solar heat fluxes.

Fig. 1.8 shows the dipole mode index. The dipole mode index is the difference in average SST anomaly between the eastern and western Indian Ocean. To study the DMI we have used the temperature difference between box-1 (50°-70° longitude and 10°S-10°N latitude) and box-2 (90°-110°E longitude and 10°S-Equator). Expt-1 reproduces the DMI index quite well, probably partly because of the relaxation to observed Reynolds SST, as explained above.

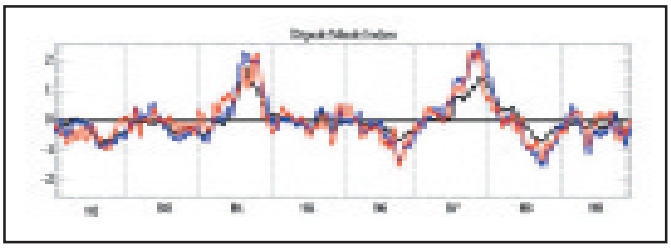

Fig. 1.8 Dipole mode index (Reynolds in Red, Expt-1 in blue and Expt-2 in black).

Expt-2 also performs quite well, despite its very crude parametrisation of the fluxes and no relaxation to SST. This shows that the wind variations explain a large part of the variance associated to dipole variability and that flux interannual variations, although important (as seen above), are not the primary driving factor of interannual SST variability.In this preliminary study we have attempted to analyse the OPA model outputs to study the SST variability of the Indian Ocean on intraseasonal time scales and compare them with observations.

C Kalyani Devasena (C-MMACS), Jérôme Vialard (LODYC, France)

1.4 Study of Sea-viewing Wide Field-of -View Sensor (SeaWiFS) data using SeaDAS

The SeaWiFS Mission is a part of NASA's, that is designed to look at our planet from space to better understand it as a system in both behavior and evolution. The purpose of the Sea-viewing Wide Field-of-view Sensor (SeaWiFS) is to provide quantitative data on global ocean bio-optical properties to the Earth science community.

Subtle changes in ocean color signify various types and quantities of marine phytoplankton (microscopic marine plants), the knowledge of which has both scientific and practical applications. The main aim of SeaWiFS project is to develop and operate a research data system that will process, calibrate, validate, archive and distribute data received from an Earth-orbiting Ocean color sensor.

This data set consists of satellite measurements of global and Regional Ocean color obtained by the SeaWiFS sensor, in orbit on the orbview2 platform. The concentration and predominant identity of substances and particles in the euphotic (lighted) zone of the upper ocean influences the apparent color of the ocean, which can range from deep blue to varying shades of green and ruddy brown. Living Phytoplankton, (which contain chlorophyll and associated photosynthetic pigments), inorganic sediments, detritus (particulate organic matter), and dissolved organic matter all contribute to the color of the ocean.

There are two distinct types of SeaWiFS data LAC (Local area coverage) and GAC (Global area coverage). GAC data is obtained at 4km.resolution over world ocean LAC data is obtained 1km resolution over the global oceans. SeaWiFS data is archived according to the standard remote sensing definitions of Level 1a, 2 and Level 3 data. Level-1a product is generated from Level-0 data files (raw radiance counts from all bands along with the spacecraft and instrument specifications) and so on. Level-1a data consists of raw radiances measured at the satellite and also includes calibrations and navigational data along with selected instrument and spacecraft telemetry. Level2 consists of derived geophysical parameters produced using level-1a radiances as input data. Level-3 is global gridded data that has been statistically collected weekly, monthly and yearly at resolution of 9km on the global oceans. All these Seawifs data archived in the form of HDF.

HDF is a self-describing, platform independent format, which has efficient capacity of storing large datasets. It is possible to store different forms of data like symbolic, numerical and graphical data within a HDF file by using appropriate HDF data structures. HDF data structures; Raster images (8-bit and General Raster)

and Palette are stored in scientific data format. HDF can be viewed at several interactive levels. At its lowest level, HDF is a physical file format for storing scientific data. At its highest level, HDF is a collection of utilities and applications for manipulating, viewing, and analyzing data stored in HDF files. HDF application program interfaces are categorized into multiple interfaces and single file interfaces. The multiple interfaces provide simultaneous access to several HDF files from within an application, where as single file interface does not support this feature. These interfaces are designed for direct file Input/ output of data streams, error handling and memory management and physical storage.

In order to Study and analyze these SeaWiFS data SeaDAS software was used. SeaDAS is a comprehensive image analysis package for the processing, display and quality control of all SeaWiFS data products (L0, L1A, L1B, L2, L3, Binned, L3 SMI, L1A-, L2-, L3- Browse) and ozone data. It has the capabilities for processing CZCS,

ADEOS/ OCTS and MOS data: Using this software one can examine the data image around a specified location, plot histograms, can extract ASCII and BINARY outputs at a region of interest. shows the Level-3 data obtained from SeaWiFS for Indian Ocean.

Several SeaDAS functions were used, programs were written to retrieve monthly average values of chlorophyll in the region [40-100E & 0-27N] at a station in the Indian Ocean.

Buoy data on oxygen procured from NIOT at 4 stations in Indian Ocean. At these four stations in Indian Ocean seasonal variations of chlorophyll values and oxygen data were analyzed.

(Jyoti Ranjan Nayak, M R Sridhar, M K Sharada)

1.5 Zonal Variations of Sea Level Over Indian Ocean Using Altimeter Data

While seasonal cycles in sea level are expected due to seasonal variabilities in the primary driving forces of ocean motion, cycles have been difficult to measure. The variations in sea level as a function of time observed by the altimeter (after due correction) are due to the temporal variability of the topography, induced primarily by currents and winds. Hence the sea level variations obtained from altimetric satellites can also be used for studies of current variability. Monthly sea surface topography maps of the Indian Ocean published from NOAA on a monthly basis in the monthly climatic diagnostic bulletins using Geosat altimeter data on a 1^0 latitude grids have been used in the present study.

Zonally averaged sea level drawn with latitude versus time for the entire 4.5 years Geosat period is shown in Fig. 1.9. Zonally averaged sea level is more in the equatorial Indian Ocean compared to the north and south of it during the southwest monsoon and vice versa during the nonmonsoon months. The Wyrtki jet starts during May resulting in the piling up of water at the eastern end of the Equatorial Indian Ocean basin. Due to this eastward flow, the sea level goes down at the western end.

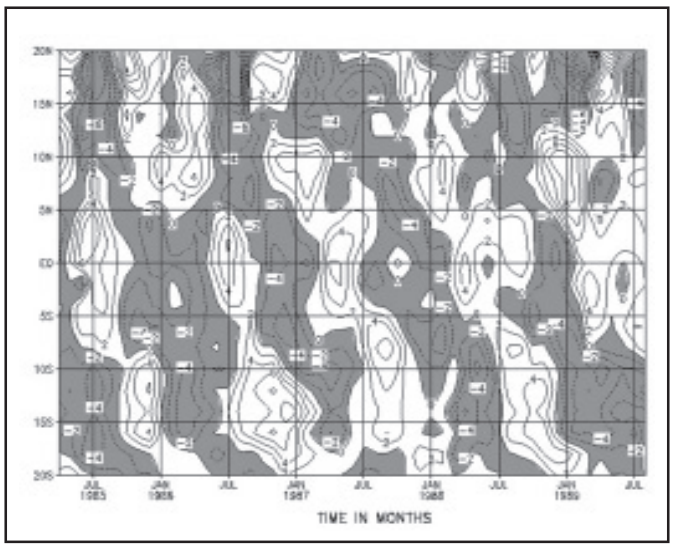

Fig. 1.9 Time-latitude plot of zonally averaged sea level derived from geosat altimeter data for 4.5 years in each 1° latitude band.

The overall rise in the sea level goes down at the western end. The overall rise in the sea level is more compared to the fall in sea level. Hence the latitudinal average of sea surface elevation is more over this region. This additional water in the Equatorial Indian Ocean is drawn from north and south and hence the sea surface elevation goes down at both sides of the Equatorial Indian Ocean. Sea surface height in the Equatorial Indian Ocean is more during the monsoon months due to the piling up of water at the eastern end as explained earlier. A southward increase in sea level is likely to result in the norhtward currents due to the increase in this sea surface elevation. In the equatorial belt the sea surface elevation. In the equatorial belt the sea surface height is more during May-October in almost all the years, the strech in time varying from year to year. The duration is longer in 1988 (a good monsoon year) compared to 1987 (a bad monsoon year). Similar

alternate bands of positive and negative sea surface heights are observed in the northen and southern parts of the Indian Ocean with an opposite phase.

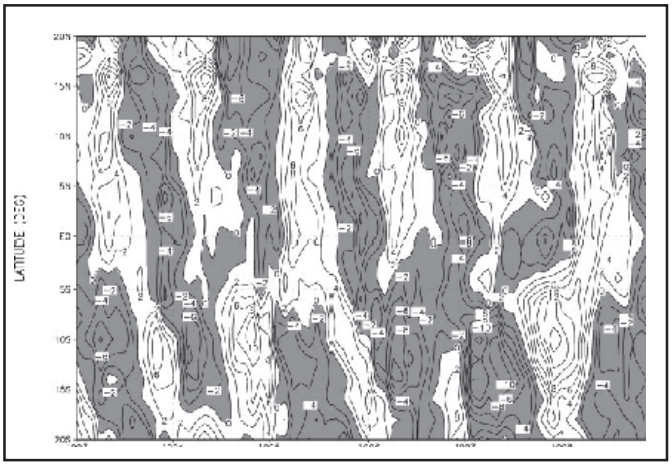

Fig. 1.10 Time-latitude plot of zonally averaged sea level derived from T/P altimeter data for 6 years in each 1° latitude band.

Fig. 1.10 shows the latitude time structure of he zonally averaged sea level for the period 1993-1998 using gridded sea surface height data.

(C Kalyani Devasena, P S Swathi)

1.6 Oxygen Profiles in Upper Ocean: Comparison of Model and Data

Dissolved gases like carbon dioxide and oxygen play a significant role in the oceanic biogeochemical cycles. A study was carried out on the role of oxygen in the marine biogeochemical cycle. Various processes influencing the oxygen distribution were incorporated in the 1D model of biogeochemical cycles developed at LODYC, France. The biogeochemical model consisting of six components (Nitrate, Ammonium, Phytoplankton, Zooplankton, Detritus, Dissolved organic matter) was applied to carry out model simulations at DYFAMED station in NW Mediterranean Sea for the years 1995 to 1997. Two forms of Nitrogen, Nitrate and Ammonium allow the estimation of new and regenerated production. The sources of export flux are zooplankton mortality and detrital sedimentation feed the export flux, and the winter mixing of accumulated semi refractory Dissolved Organic Matter (DOM) is associated with the dissolved export flux, which can be the major export flux in the Mediterranean Sea. Compared to other complete models, bacterial production is not explicitly taken into account. The coupling between nitrogen and carbon cycles, and nitrogen and oxygen use mostly Redfield ratio considerations, whereas C/Chl ratio is assumed to be constant.

The biogeochemical model is embedded in a 1D physical model, which simulates the time evolution of temperature, salinity and turbulent kinetic energy. The only dynamic process which is taken into account is vertical diffusion. The simulation is forced by the ECMWF atmospheric data, which give the wind stress and heat fluxes every 6 hours. The diffusion coefficient of vertical mixing for the biogeochemical tracers is the same as that of temperature and salinity. The model simulates the tracer evolution from the surface to 200m, with a vertical resolution of 5m, the bottom layer being closed.

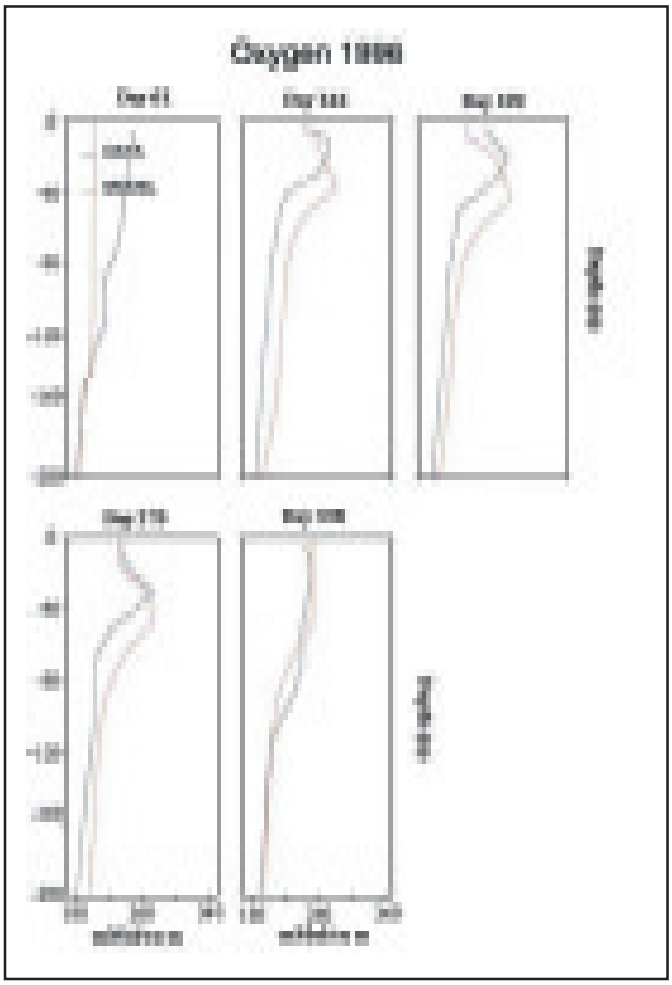

Fig. 1.11 Comparison of vertical profiles of oxygen obtained from model simulations with observations.

At the air-sea interface, fluxes for CO_2 and O_2 are considered. Nitrogen is not conserved in the system, since a fraction of the zooplankton mortality is instantaneously exported out of the system. Like temperature and salinity, dissolved tracers like nitrate, dissolved organic nitrogen, dissolved inorganic carbon, dissolved oxygen and alkalinity are

restored in winter towards climatological homogeneous profiles. The carbonate equations, which give the partial pressure of CO_2 in terms of Dissolved Inorganic Carbon (DIC) and alkalinity, are obtained from Dickson and Millero, with CO_2 solubility given by Weiss. The air-sea CO_2 fluxes are computed from wind speeds using Liss and Merlivat relationship. The partial pressure of O_2 is obtained with O_2 solubility as a function of temperature and salinity. Computations show that after two years, the system approaches an annual cycle of periodic steady state. Therefore, the standard run is made of three repeated 1995 years, followed by the years 1996 and 1997 : only the three last years of the run are analysed.

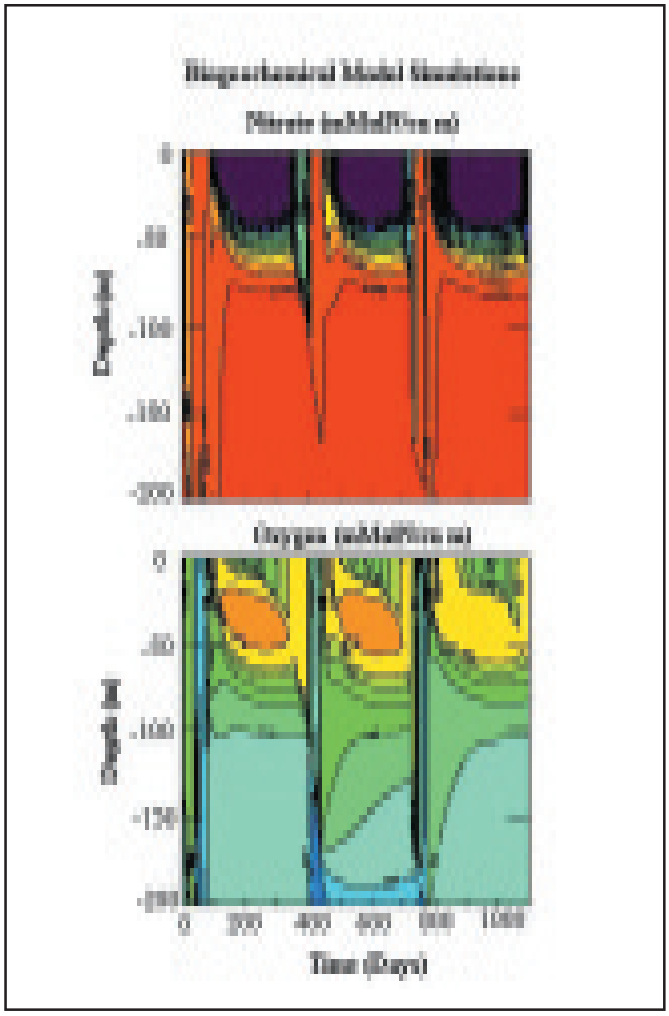

Fig. 1.12 Time evolution of oxygen and nitrate in the water coloumn for three years.

The biogeochemical processes influencing the concentration of oxygen are the primary production, detrital decay, oxidation of dissolved organic matter, nitrification, and respiration. During photosynthesis by the phytoplankton, carbon is consumed and oxygen is released. This is the only source of oxygen in the ocean. There is consumption of oxygen due to respiration of phytoplankton, zooplankton and animals at the higher trophic level. Oxygen is consumed for the process of nitrification, in which bacteria converts ammonium to nitrate. Oxidation of DOM by bacteria and detrital decay also consumes oxygen. All these processes were considered to formulate the model for determining the concentration of oxygen in the water column. Denitrification process is not considered in our analysis since it is not a significant process in Mediterranean sea. To calculate the oxygen concentration, values of various ratios like C/N, O/N are required. Two values of Redfield ratio (8.625 and 10.75) for O/N were considered. Sensitivity of the model results for different Redfield ratios of oxygen was studied.

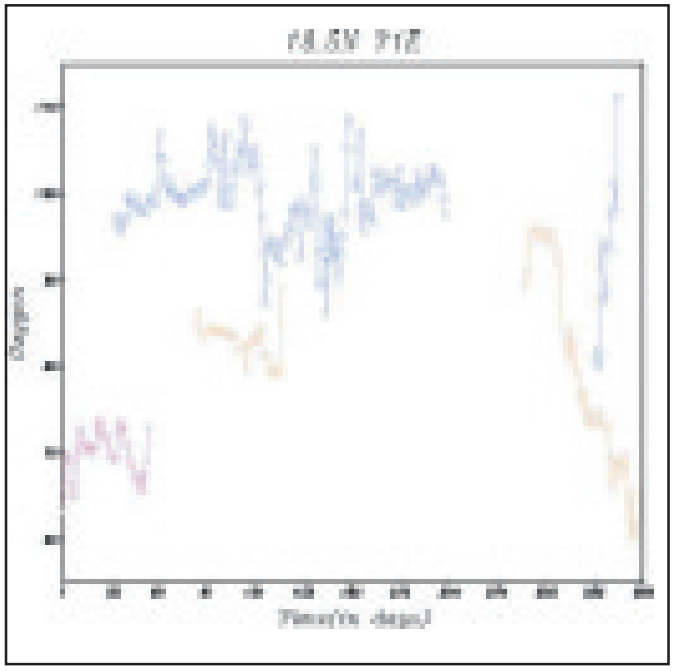

Fig 1.13 Seasonal variation of dissolved oxygen obtained from buoy data.

Numerical simulations were carried out for seven variants of the model. The basic aim of the model simulation is the validation of the model against oxygen data obtained at DYFAMED station. Validation can be only qualitative since the temporal coverage of the various profiles is no better than monthly. Figure 1.11 compare several profiles of oxygen during 1995, 1996 and 1997. The model results differ from the data in the details. In most of the simulation results, the maximum of oxygen is deeper compared to the observations. The oxygen maximum zone is broader in the model results than in the observed profiles. In all cases of model runs, below 100m upto 200m, concentration of oxygen remains constant. Model

simulations showed that oxygen concentration decreases when Redfield ratio for oxygen is decreased. In many of the cases, the model run with lower Redfield ratio for the source term and the higher Redfield ratio for all the sink terms of oxygen compared well with the maximum oxygen concentration observed in the data, but the depth of the oxygen maximum was deeper compared to the observations. To understand the factors responsible for change in the depth of oxygen maximum, comparisons of profiles of nitrate, density and temperature with the data was carried out. Nitracline and pycnocline obtained in the model simulations compared well with the observations in most of the cases. The profiles of chlorophyll were studied carefully for years 1995, 1996 and 1997, for all the cases of model simulations. Most of the model simulations showed the depth of the chlorophyll maximum is same as that seen in the data and hence, vertical distribution of chlorophyll can not explain the deeper oxygen maximum in the simulation results. Since the observations of DIC were not available for the years 1995-97, the simulation results of 1996 and 1997 were compared with observed DIC profiles of 1998 and 1999. These comparisons did not yield any hints for understanding the model better. In all the model runs, time evolution of different components of the model, the fluxes of oxygen, vertical balance of the oxygen fluxes averaged over first 100m and profiles of different fluxes of oxygen on different days of the year when the observation data are available, were examined. Time evolution of Oxygen and Nitrate in the water column over three years (Fig.1.12) shows that the depth at which oxygen is maximum corresponds to the depth where nitrate is minimum, implying that photosynthesis is maximum at that particular depth. Also, time evolution of oxygen concentration is found to be sensitive to the Redfield ratio of oxygen. Vertical balance of oxygen fluxes over first 100m is not qualitatively very different from each other for different model runs. The profiles of different fluxes of oxygen show that the diffusion of oxygen dominates during the summer months and the biological fluxes dominate during the winter. For the model runs, in which different Redfield ratios were considered for primary production due to ammonium and nitrate, the chlorophyll concentration averaged over first 110m compared well with that of the observations during 1996. Both qualitative and quantitative differences were seen when oxygen concentrations averaged over first 110m obtained from a model simulation was compared with that of observed data. Average values of temperature over first 110m, obtained from the model compared well with observations during all the three years. (This work was carried out under the IFCEC programme)

The results obtained for the different model runs, show that model needs some modifications in the dynamics of the model and resolution of model computations. Some improvements in the biology of the model are required since bacteria is not included explicitly in the model which plays a major role in the biogeochemical processes influencing the oxygen concentration in the ocean like oxidation of DOM, detrital decay, nitrification etc. The biogeochemical model proposed by Fasham which includes microbial loop, is being incorporated in the 1D model of LODYC. This model will be applied to the Indian ocean. The buoy data on dissolved oxygen at four stations in Indian ocean are procured from NIOT, Chennai and will be used for validating the water column model. Fig.1.13 shows the seasonal variation of dissolved oxygen obtained from buoy data. Detailed study of different water column models is being done to introduce some modifications in modelling the dynamics to capture the vertical structure. Also, a study of the forcing functions required for the 1D model simulations for the Indian Ocean is being carried out.

(M K Sharada, Laurent Memery, K S Yajnik*
**LODYC, France)*

1.7 Oceanic Response to Wind Forcing at Different Frequencies

At C-MMACS efforts are on to develop a coupled general circulation model (CGCM) by coupling the Modular ocean model (MOM) and the atmospheric general circulation model of Laboratory for Dynamic Meteorology, Paris. As a first and important step towards this a set of simulations with MOM was carried out to determine whether and how

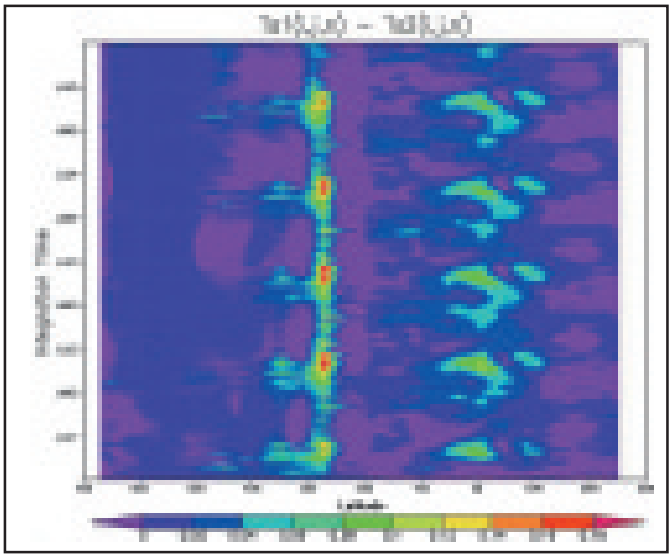

Fig. 1.14 Time-longitude structure of ΔT over the equator.

the ocean responded differently to wind forcing applied at two different frequencies viz., 6hours and 24 hours. For the present stand-alone phase the wind fields are taken from the National Centre for Environmental Prediction (NCEP) data sets available at 6 hourly and daily intervals; in the coupled model, of course, these wind fields will be derived from the atmospheric component.

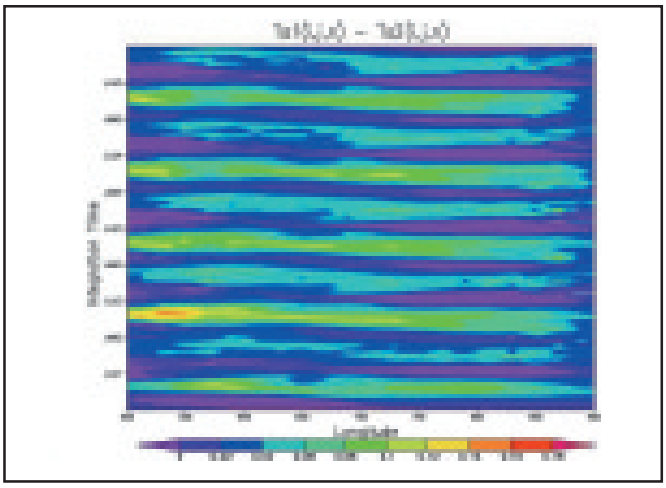

Fig. 1.15 Time-latitude structure of ΔT over 60^0 E.

The simulations were carried out on a uniform horizontal grid of 2×2 degree with 13 vertical levels; the level nearest to the surface is at 5m depth. The model was initialized with Levitus climatology and a spin-up period of 3 years was allowed for the model to achieve dynamic equilibrium. For each set (6 hourly and daily) of wind forcing, the model was integrated for 2 years beyond the spin-up period. The NCEP wind fields, both zonal and meridional components, used in the model are for the year 1998 with a grid spacing of 2X2 degree. Wind stress is calculated from this data using speed-dependant drag coefficient. A considerable difference in the results was noticed when we replaced drag coefficient with speed-dependant drag coefficient. constant Sea surface temperature is used as a restoring force in the model, using the monthly average data from Atmospheric Model Intercomparison Project(AMIP)

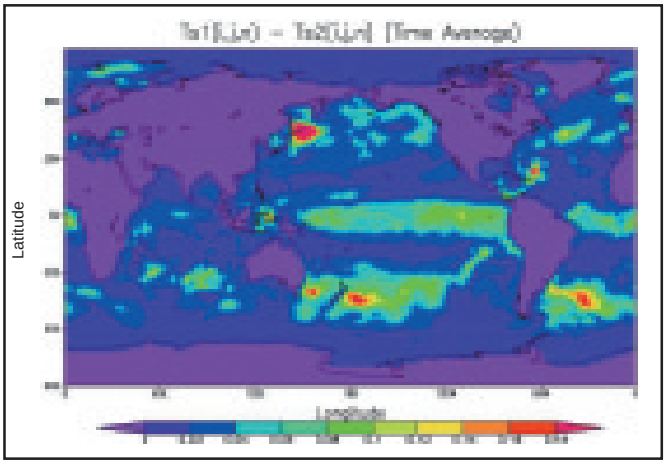

Fig. 1.16 Latitude-longitude structure of average ΔT.

To analyze the simulations we have defined the following quantities.

$$\Delta T = T_{S1}(i,j,n) - T_{S2}(i,j,n)$$

where T_{S1} and T_{S2} represents the simulated oceanic sub-surface temperature at 5 m depth with daily wind forcing and 6 hourly wind forcing respectively. i, j, n are longitude, latitude and time respectively. The formula for speed-dependant drag coefficient is as follows.

Cd = 0.00218 for U < 1
= (0.62+1.56/U) × 0.001 for 1 < U < 3
= 0.00114 for 3 < U < 10
= (0.49 +0.065 × U)×0.001 for U > 10

Where U is the wind speed in m/s.

Figure 1.14 shows the Time-Longitude Structure of ΔT at the equator for two years over 50^0E to 90^0E. Similarly Figure 1.15 shows the Time-Latitude Structure of ΔT over 60^0E. While the values are small, there exists a systamatic and persistent difference between simulations with two wind forcings.

Figure 1.16 shows the latitude-longitude structure of the time average (over 2 simulation years) of ΔT. It is clear that the oceanic response to the different wind-forcings have strong spatial dependancies. These results will provide a background for investigation with wind forcings from atmospheric models.

(P Goswami, P Rajeevan)

1.8 Oceanographic Data Analysis

Data analysis is of great importance in the area of Oceanographic and atmospheric sciences. The datasets containing information at various spatial and temporal scales for the ocean are obtained from different sources like satellites, buoys, ship, station, radar etc. Satellites provide information on a broad range of geophysical quantities such as the vertical distribution of atmospheric temperature, moisture, clouds, winds, atmospheric gases, sea surface temperatures, ocean color etc,. These data archived from the satellite have more advantages than the data archived from the other resources because actual oceanographic quantities are derived using sophisticated retrieval algorithms, and are available for large areas over long periods of time.

Oceanographic data can be archived different formats: a) Character format b) Native format c) packed binary format or scientific data formats.

Standard scientific data formats include

1. GRID in binary (GRIB): used for 2-dimensional oceanographic data.
2. Common Data Formats (CDF): for storing, manipulating and accessing multidimensional datasets.
3. Network Common Data Formats (NetCDF): Interface for array oriented datasets.
4. SD2 (Station Data): Useful in physical-chemical oceanographic data recorded at discrete depth levels.
5. UBT: format for temperature profile data (temperature vs. depth) from the mechanical bathy thermographs.
6. HDF: Multiobject file format for sharing Scientific data in a distributed environment.

Most of the database management systems in the past do not have capability to analyze the huge amount data in the form of satellite images, the scientific model outputs, and long term global observations. We have developed the software package using 'C' language and NetCDF interface for converting gridded sea level data derived from Topex altimeter data of the Indian Ocean [40-100E and 0-27N]. To visualize the NetCDF files Ferret and Grads software packages were used.

(Jyoti Ranjan Nayak, M R Sridhar, C Kalyani Devasena)

1.9 Modelling of Soil Moisture Variability

Soil moisture plays an important role in various hydrological processes acting over a range of spatio-temporal scales, like partitioning of rainfall into infiltration and runoff, partitioning of net radiation into sensible and latent heat. Knowledge of soil moisture is of crucial importance for irrigation scheduling, precision farming, groundwater recharge, hydrological modelling and flood forecasting. Exchange of moisture flux between land surface and atmosphere is the major link of interaction between hydrological and atmospheric processes. Soil moisture dynamics model based on highly nonlinear Richards's equation that describes moisture content in the unsaturated zone has been developed at C-MMACS as prelude to develop coupled atmospheric-hydrologic modelling platform. The model, which assumes the entire region as multi layered vertical column, solves the Richards equation numerically and assumes exponential decrease type of saturated hydraulic conductivity function. The model was forced with rainfall as surface boundary condition. The observed vertical soil moisture profiles shown in Fig.1.17, for Orissa-1995-Dec, Telangana-1989-Dec and West Rajasthan-1996-Jan were used as initial conditions.

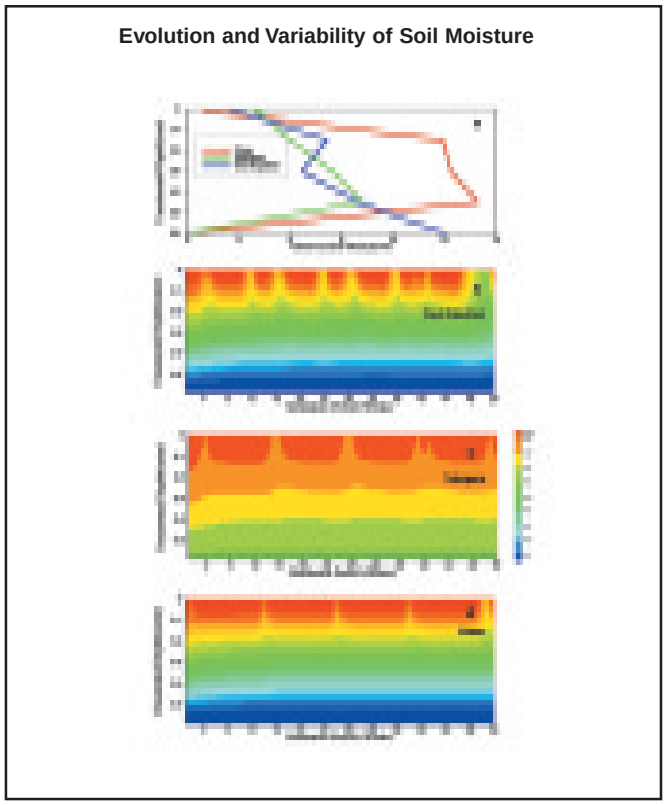

Fig. 1.17 Time-depth structure of soil moisture simulated. The top panel shows the initial profiles taken from observed weekly profiles for different stations. The subsequent panels show soil moisture for different basins.

Simulation experiments were carried out up to one hundred and ten weeks and the numerical scheme (Leapfrog) has been found to be stable. Fig.1.17 (b)(c) and (d) shows experimental simulation of the evolution of soil moisture variability for those representative regions. Simulation results show more pronounced soil moisture variability closer to surface than at deeper layers reflecting significant impact of rainfall event nearer to surface and its gradual attenuation towards deeper layers. M odel simulated relatively higher moisture content for Telangana region over larger depth compared to Orissa and West Rajasthan, this needs to be further investigated in terms of region specific soil physics, since, current simulation experiments predominantly reflects rainfall induced moisture variability. Markedly distinct temporal variability of moisture over the entire simulation period in all the three different regions again seems to reflect prevailing rainfall pattern in these regions over the period.

(P Goswami and S Himesh)